Journal of Magnetic Resonance 208 (2011) 49–57

Contents lists available at ScienceDirect

Journal of Magnetic Resonance

journal homepage: www.elsevier.com/locate/jmr

Selective detection of hyperpolarized NMR signals derived from *para*-hydrogen using the Only *Para*-hydrogen SpectroscopY (OPSY) approach

Juan A. Aguilar [a,*], Ralph W. Adams [a], Simon B. Duckett [a,*], Gary G.R. Green [b], Rathika Kandiah [a]

[a] Department of Chemistry, University of York, Heslington, York, YO10 5DD, UK
[b] York Neuroimaging Centre, The Biocentre, York Science Park, Innovation Way, Heslington, York, YO10 5DG, UK

ARTICLE INFO

Article history:
Received 23 August 2010
Revised 4 October 2010
Available online 8 October 2010

Keywords:
para-hydrogen
Double quantum (*DQ*)
Zero quantum (*ZQ*)
Multiple quantum
Pulsed field gradients
Coherence order selection
Signal Amplification By Reversible Exchange (SABRE)
Solvent suppression
Hyperpolarization
Hydrogenation

ABSTRACT

A new family of NMR pulse sequences is reported for the recording of *para*-hydrogen enhanced NMR spectra. This Only *Para*-hydrogen SpectroscopY (OPSY) approach uses coherence selection to separate hyperpolarized signals from those of fully relaxed and thermally equilibrated protons. Sequence design, performance, practical aspects and applicability to other hyperpolarization techniques are discussed.

1. Introduction

It is well established that greatly enhanced ^{1}H NMR signals can be obtained from molecules that are formed by the addition of hydrogen in the *para*-nuclear spin state [1–3]. Since it's inception, the use of *para*-hydrogen induced polarization (PHIP) as a tool in a range of applications spanning high resolution NMR spectroscopy and MRI has grown substantially as the benefits of the approach have become more widely recognised [4,5].

The signal enhancements PHIP provides have been used extensively to detect elusive reaction intermediates based on metal dihydrides by NMR spectroscopy [6,7]. It has also been used to generate hyperpolarized organic molecules by hydrogenation of unsaturated substrates [5]. By considering the time evolution of the associated spin states information has been elucidated about the mechanism of their formation [8]. Furthermore, polarization transfer techniques have been used to sensitize the detection of spins coupled to the former *para*-hydrogen nuclei [4,9,10]. Recently PHIP has been used to detect metal complexes through the incorporation of *para*-hydrogen into groups such as $CHPhCH_2Ph$ which are bonded to the metal [11] and has been used to record ultra-fast ^{13}C-MR images in such hydrogenation products [12,13].

Dynamic Nuclear Polarization (DNP) [14] is currently one of hyperpolarization's most successful approaches having been shown to increase the level of ^{13}C polarization in pyruvic acid to 64% [15]. Golman has used the differences to good effect to produce ^{13}C-MR Images of animals injected with ^{13}C enriched hyperpolarized materials such as pyruvate, where contributions from the background are minimal because of the vast signal amplification of the hyperpolarized substrate [16]. Due to the low natural abundance and inherent sensitivity of ^{13}C, only the hyperpolarized, ^{13}C-enriched, molecules contribute to the images. Regions, where pyruvate was metabolised were consequently made visible with real-time MRI as both substrate and alanine metabolite remain hyperpolarized. No manipulation of the ^{1}H magnetization was performed in these studies and the images rely on the absence of a background ^{13}C signal. *Para*-hydrogen has also been used to polarize several materials by the hydrogenative route, including fumarate and succinate, to facilitate ^{13}C based MRI [5,17].

In a recent development, it has been demonstrated that it is possible to sensitize the NMR signature of a molecule through its interaction with *para*-hydrogen without the need to formally

* Corresponding authors. Present address: School of Chemistry, University of Manchester, Oxford Road, Manchester, M13 9PL, UK (J.A. Aguilar). Fax: +44 1904432516.
E-mail address: sbd3@york.ac.uk (S.B. Duckett).

1090-7807/$ - see front matter © 2010 Elsevier Inc. All rights reserved.
doi:10.1016/j.jmr.2010.10.002

incorporate it into the molecule of interest [18,19]. This result is achieved by creating a coupled spin system in low magnetic field connecting nuclei in *para*-hydrogen with those in the molecule to be polarized [16]. This process occurs within a suitable metal complex, and on dissociation of the molecule its enhanced NMR signature can be read. This technique has been termed 'Signal Amplification By Reversible Exchange' or SABRE.

Para-hydrogen enhanced NMR signals have also been monitored in real-time to study reaction mechanisms and directly obtain kinetic information for reaction intermediates [20,21]. For this type of study, ^{1}H magnetization is usually detected and consequently background signals are present in the resulting spectra requiring identification. Even if the signals for a reaction intermediate are enhanced by 1000 fold, if they are formed at only 1% of the catalyst concentration and there is a 100 fold substrate excess, the net background to hyperpolarized signal ratio is still only 10:1. This demonstrates the likelihood that there will be significant contributions to the NMR spectrum from the thermally equilibrated signals with the potential of overlap meaning that the PHIP effect itself may still be masked by other signals such as that due to the solvent.

This work focuses on exploiting the inherent differences between molecules that have been formed by incorporating *para*-hydrogen and those that exist with a thermally equilibrated spin distribution. It also demonstrates that similar observations can be made for substrates polarized via the SABRE method. In addition to the increase in signal intensity that can be observed for these molecules, they exist in a defined spin state that can be manipulated through the use of radiofrequency (r.f.) pulses and pulsed magnetic field gradients (PFGs). This allows them to be distinguished from their non-hyperpolarized counterparts.

A traditional route to the separation of signals derived from *para*-hydrogen and those of the background has been based on exploiting differences that exist between the two spin states, $2I_zS_z$ and $I_z + S_z$. In practice this has been achieved by using alternate addition and subtraction of ^{1}H NMR experiments recorded using $-\pi/4$ and $3\pi/4$ pulse angles. This approach was first proposed for Chemically Induced Dynamic Nuclear Polarization (CIDNP) [22]. For systems with a rapidly changing chemical composition this method is inefficient and consequently when hyperpolarized signals overlap with other signals in the sample they still may be concealed. In spite of this problem, it has been used successfully on several occasions in conjunction with *para*-hydrogen [23–25]. A robust method that mimics this approach is clearly desirable for ^{1}H based MRI measurements using *para*-hydrogen enhancements.

By employing fully deuterated substrates we have exemplified how thermally equilibrated signals can be eliminated. For example deuterated diphenylacetylene has been used to prevent dynamic range and overlap problems in a number of high resolution NMR studies [26,27]. However, the catalyst and residual protio solvent were found to contribute to the observed signals as they are sources of non-hyperpolarized protons. Furthermore, even when using fully deuterated reagents and catalysts, the hydrogenation reaction itself will produce protio molecules that give rise to thermally equilibrated signals which compromise the results provided by such experiments.

One other way in which we have separated key NMR signals is through the use of two-dimensional experiments such as COSY or HMQC. However, the COSY approach does not address the dynamic range issue and as with all multidimensional techniques, can be time consuming.

Here we describe more fully the *Only Para-Hydrogen SpectroscopY* (OPSY) approach that we have briefly communicated [28]. This method selects *para*-hydrogen derived hyperpolarized signals through a PFG based quantum coherence filter. As a one-dimensional technique it achieves selection in a single transient. Due to its ability to convert different spin states into observable magnetization the OPSY approach has the potential to become a background suppression technique that enables the monitoring of *para*-hydrogen based reactions in real-time using protio rather than deuterio solvents. We therefore expect it to become a building block for both NMR and MRI procedures in the future. In this contribution we discuss and exemplify the method and present additional NMR sequences that utilize the approach. Specific details about sequence development, its performance and implementation are discussed and its utility with SABRE established.

2. Material and methods

Pure *para*-hydrogen was prepared by cooling hydrogen gas to 20 K in the presence of a charcoal catalyst [6]. [Ir(CO)(P(*p*-$MeC_6H_4)_3)_2$Cl] was prepared using a method adapted from the literature [29,30] (See Supplementary Information). *Sample A* contained 1 mg of [(1,5-cyclooctadiene)Rh(dppp)]BF_4 (where dppp is *bis*-diphenylphosphinopropane), 40 μL of penta-1,3-diene, 10 μL of pentane, 2 mg of cholesterol acetate, 3 mg of strychnine in 0.6 mL of methanol-d_4. *Sample B* contained 3 mg of [Ir(CO)(P(*p*-$MeC_6H_4)_3)_2$Cl] and 20 μL of pyridine in 0.6 mL of C_6D_6. *Sample C* contained 3 mg of [Ir(CO)(P(*p*-$MeC_6H_4)_3)_2$Cl] in 0.6 ml of C_6D_6, All three samples were degassed thoroughly prior to the addition of 3 atm of *para*-hydrogen. *Sample D* contained 5 mg of Crabtree's catalyst, [Ir(cod)(PCy_3)(py)][BF_4] which reacts with 25 μL pyridine and 3 atm of *para*-hydrogen in low magnetic field to produce [$Ir(H)_2(PCy_3)(py)_3$][BF_4] and hyperpolarized pyridine.

For a typical experiment with *para*-hydrogen the sample was placed in an NMR tube fitted with a J. Young tap inside a nitrogen glove box and the solvent added by means of vacuum transfer. The sample was then degassed before being placed inside the NMR spectrometer. The shims were optimized and the ^{1}H $\pi/2$ pulse calibrated. The acquisition times used provided sufficient spectral resolution to prevent cancellation of anti-phase signals yet were short enough to maximize the amount of signal recorded per unit time with common values between 300 and 500 ms. Half-sine PFGs with a maximum strength of 53 G cm^{-1} were used with a recovery delay of 500 μs. The gradient durations were increased when necessary to enable signal suppression within a range of durations from 1 to 3 ms.

3. Theoretical approach

Experiments with *para*-hydrogen are generally performed in one of three ways to take advantage of either or both of the ALTADENA or PASADENA effects [4,21,31,32]. To produce the so called PASADENA enhancement the reaction is started and performed inside the magnet. To conduct an ALTADENA-type experiment, an NMR tube fitted with a Young's style tap and charged with the reaction mixture is first pressurized with *para*-hydrogen, then shaken and introduced into the magnet. However, as the reaction still proceeds inside the magnet, the hyperpolarization route changes instantaneously from ALTADENA to PASADENA for any species formed at high field. The ALTADENA signals remain detectable until depleted by longitudinal relaxation. These two situations are reflected in the following descriptions which consider the resulting time-dependent density matrix for the two ^{1}H atoms resulting from addition of a molecule of *para*-hydrogen to an isolated non-symmetric spin system comprising I and S [33].

$$\rho(t) = 1/2(2I_zS_z + a(t)(2I_xS_x + 2I_yS_y) + b(t)(2I_yS_x - 2I_xS_y) + c(t)(I_z - S_z)) \quad (1)$$

In Eq. (1), the coefficients $a(t)$, $b(t)$, and $c(t)$ are time-dependent functions that define the state of the spin system at time t for the specified spin angular momentum product operators (see Sorensen

et al. [34]). After product formation, the $a(t)(2I_xS_x + 2I_yS_y)$ and $b(t)(2I_yS_x - 2I_xS_y)$ terms evolve, inter-converting between $c(t)(I_z - S_z)$ and each other. The nature and extent of this inter-conversion is dependent upon the chemical shifts and scalar coupling of the two nuclei. Time averaging the coefficients during the reaction time prior to the interrogating, r.f.-pulse simplifies the expression into that shown in Eq. (2). This reflects the situation that is achieved after adiabatic transfer of the sample to high field (the ALTADENA effect) [32,33].

$$\rho = 1/2(2I_zS_z) \pm 1/2(I_z - S_z) \quad (2)$$

In contrast, when the reaction occurs at high field only the longitudinal 2-spin order term, $2I_zS_z$, prevails. The resultant PASADENA derived magnetization is shown in:

$$\rho = 1/2(2I_zS_z) \quad (3)$$

In the third approach, the SABRE method, *para*-hydrogen adds to a metal catalyst which also contains a substrate such that the *para*-hydrogen and substrate in the resulting complex become spin–spin coupled. At low field, polarization transfers from the *para*-hydrogen to the substrate. Subsequent dissociation of the complex yields hydrogen and hyperpolarized substrate. The sample is then transferred to the measurement field for interrogation. For a substrate based on a two spin system, $R + T$, this approach results in the formation of magnetization including $f(t)R_z$, $g(t)T_z$, and $h(t)\ 2R_zT_z$. The sign and magnitude of the coefficients $f(t)$, $g(t)$, and $h(t)$ are determined by the evolution of the magnetization from *para*-hydrogen that results during the sample preparation step and is controlled by the interaction time, the coupling framework, and the chemical shift difference between the interacting groups [15].

A traditional *para*-hydrogen based ^{1}H NMR experiment detecting hydrogenated products is usually performed using a $\pi/4$ tip angle [2]. This produces optimum results with the initial term $½(2I_zS_z)$ that is present in both ALTADENA and PASADENA experiments. ALTADENA-type experiments can also be viewed after a $\pi/2$ pulse since it is the effect on both the $2I_zS_z \pm (I_z - S_z)$ terms with the single spin terms contributing to the observed spectrum. With PASADENA no signal is seen under this condition. Consequently the appearance of the resultant NMR spectra depend strongly on the tip angle used [32,33]. The key to a successful *para*-hydrogen experiment is to observe the spin system before these terms can relax into thermal equilibrium magnetization associated with the more usual $I_z + S_z$ terms.

This process, however, is complicated by the fact that when the sample is first introduced there is an element of sample instability due to the shaking of the NMR tube to dissolve the *para*-hydrogen. Both convection and turbulence in the sample can then cause inefficient signal cancellation or signal loss in NMR experiments that rely on phase cycling or pulsed field gradients for coherence selection. This problem is exacerbated at the point of sample introduction as the concentration of reactants and the purity of *para*-hydrogen are at their maximum. Hence at this time the strongest signals might be expected for any reaction intermediates, and related species, that are produced. Observations with *para*-hydrogen based samples are also made rapidly because the $2I_zS_z$ spin order from which the associated signal is derived is replenished throughout the reaction and thereby repeating the observation before relaxation is not essential. This means that it is simply necessary to ensure that there are sufficient freshly prepared products containing protons derived from *para*-hydrogen for detection. By using fast repetition rates the signals associated with non-hyperpolarized products are attenuated.

In order to understand the Only*Para-hydrogen* SpectroscopY approach, the spin dynamics of the *para*-hydrogen derived systems need to be further considered. The initial two spin order term $2I_zS_z$ ($2R_zT_z$ for SABRE) yields $2I_yS_y$ after a $\pi/2(x)$ r.f. pulse which is a mixture of zero and double quantum coherences ($ZQ_x - DQ_x$)[35] that are not directly observable. These terms evolve further during a finite delay, τ, according to their frequency shifts, ω_I and ω_S, into those detailed in

$$\begin{aligned} &2I_xS_x\{1/2\cos[\tau(\omega_I-\omega_s)] - 1/2\cos[\tau(\omega_I+\omega_s)]\} \\ &\quad + 2I_yS_x\{1/2\sin[\tau(\omega_I-\omega_s)] - 1/2\sin[\tau(\omega_I+\omega_s)]\} \\ &\quad - 2I_xS_y\{1/2\sin[\tau(\omega_I-\omega_s)] + 1/2\sin[\tau(\omega_I+\omega_s)]\} \\ &\quad + 2I_yS_y\{1/2\cos[\tau(\omega_I-\omega_s)] + 1/2\cos[\tau(\omega_I+\omega_s)]\} \end{aligned} \quad (4)$$

These terms are subsequently converted by a $\pi/2(y)$ pulse into those shown in

$$\begin{aligned} &2I_zS_z\{1/2\cos[\tau(\omega_I-\omega_s)] - 1/2\cos[\tau(\omega_I+\omega_s)]\} \\ &\quad + 2I_yS_z\{1/2\sin[\tau(\omega_I-\omega_s)] - 1/2\sin[\tau(\omega_I+\omega_s)]\} \\ &\quad - 2I_zS_y\{1/2\sin[\tau(\omega_I-\omega_s)] + 1/2\sin[\tau(\omega_I+\omega_s)]\} \\ &\quad + 2I_yS_y\{1/2\cos[\tau(\omega_I-\omega_s)] + 1/2\cos[\tau(\omega_I+\omega_s)]\} \end{aligned} \quad (5)$$

Some of these terms then continue to evolve with time such that detectable coherences are created during acquisition of the FID. PFGs are used to select either the ZQ or DQ coherence pathways to produce observable magnetization that originates from the $2I_zS_z$ spin order of the *para*-hydrogen. This situation contrasts with that described earlier, where an initial $\pi/2$ r.f. pulse simply generates unobservable coherences. The pulse sequences used experimentally to implement OPSY are illustrated in Fig. 1. When the second $\pi/2$ r.f. pulse is flanked by two PFGs of ratio of 1:2, several coherences are retained at end of the second gradient, ignoring evolution during the second gradient pulse, as shown in Equation (6).

$$\begin{aligned} &1/2\ 2I_zS_z\,\pi\cos[\tau(\omega_I-\omega_s)] + 1/4\ 2I_xS_x\,\pi\cos[\tau(\omega_I-\omega_s)] \\ &\quad + 1/42I_yS_y\pi\cos[\tau(\omega_I-\omega_s)] - 1/4\ 2I_zS_x\pi\cos[\tau(\omega_I+\omega_s)] \\ &\quad - 1/4\ 2I_xS_z\,\pi\cos[\tau(\omega_I+\omega_s)] - 1/4\ 2I_yS_z\,\pi\cos[\tau(\omega_I+\omega_s)] \\ &\quad - 1/4\ 2I_zS_y\,\pi\cos[\tau(\omega_I+\omega_s)] \end{aligned} \quad (6)$$

During the acquisition I_x, I_y, S_x, S_y, I_zS_x, I_zS_y, I_xS_z, and I_yS_z are generated in differing proportions depending on the chemical shift and scalar coupling for I and S. Non-observable coherences and magnetization are also generated. Quantitative values for these are given in the Supplementary Information. This situation corresponds to the double quantum coherence selected variant and is referred to as OPSY-*d*.

Experimentally, the use of PFGs with opposite polarity produced the clearest spectra and the pulse sequence for this is depicted in Fig. 1a. In contrast, when the second $\pi/2$ r.f. pulse is

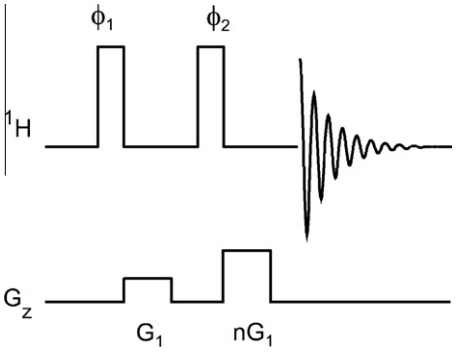

Fig. 1. *n* Quantum coherence selection based OPSY sequences. Gradient strength (G): 53 G cm^{-1}, first gradient duration for the experiment was 1 ms using a half-sine gradient with 0.5 ms stabilization delay. For the case: $n = 2$, giving a double quantum coherence selection (OPSY-*d*) the second gradient pulse duration was 2 ms; for $n = 0$, no second gradient pulse is employed.

preceded by a single PFG (i.e. gradient ratio 1:0) different coherences are retained after the second r.f. pulse, these are shown in Equation (7), and a zero quantum coherence selection form of the experiment, OPSY-*z*, is implemented. Observable magnetization is then generated during the acquisition and the coefficients for the coherences and magnetization are different to those in the OPSY-*d*. (See Supplementary Information for full analysis)

$$1/2\ 2I_xS_x\cos[\tau(\omega_I-\omega_s)]-1/2\ 2I_xS_z\pi\cos[\tau(\omega_I-\omega_s)] + 1/2\ 2I_zS_x\pi\{\cos[\tau(\omega_I-\omega_s)]+1/2\ 2I_zS_z\pi\{\cos[\tau(\omega_I-\omega_s)] \quad (7)$$

The pulse sequence for OPSY-*z* is depicted in Fig. 1b.

These two coherence pathways can be selected without retaining any signal from thermally polarized magnetization (derived from $I_z + S_z$) in a single observation. Thermal magnetization of the type $I_z + S_z$ is converted into $I_y + S_y$ by the initial $\pi/2(x)$ r.f. pulse which is then dephased by the gradients. The efficiency of the sequence can further be increased by phase cycling [36,37].

4. Performance

To assess the performance of the two OPSY sequences directly, a series of reaction samples were prepared to test a range of experimental conditions, such as protio solvent, low catalyst loading, high substrate loading and the need for a rapid reaction.

In our first sample, [(COD)Rh(dppp)]$^+$, was employed as the homogeneous hydrogenation catalyst and 1,3-pentadiene as the substrate dissolved in methanol-d_4 (*Sample A*). Signals from the hydrogenation product pentane are expected between δ 1 and 3. In order aid in the assessment of the NMR sequence's performance we added strychnine and cholesterol acetate to add to the background in this region. Field inhomogeneity effects were inadvertently introduced because of the low solubility of strychnine and its propensity to precipitate.

Fig. 2a and b shows the resultant ^{1}H NMR spectra of *sample A* obtained using a simple $\pi/4$ r.f. pulse followed by acquisition and the OPSY-*d* experiment respectively. These two NMR spectra were recorded immediately after adding *para*-hydrogen to the solution and introducing the sample. Consequently the enhanced NMR signals for the reaction products are expected to be their most intense as are the changes in their signal intensities. Similar spectra were obtained after allowing the reaction to progress for a few minutes and removing the sample from the magnet, shaking it to dissolve fresh *para*-hydrogen, and returning it to the magnet for observation (Fig. 2c, OPSY-*d*). The $\pi/4$-^{1}H NMR experiment (Fig. 2a) shows three overlapping anti-phase signals at δ 2.02 and 1.41 (1-pentene) and 1.59 (2-pentene) but contains very little evidence for the expected hyperpolarized signal of 2-pentene at δ 0.96 which confirms that it would be difficult to detect reaction intermediates robustly in such spectra. To overcome this overlap problem previously, ^{2}H-labelling of the reactants and solvent was necessary [21]. The results from the OPSY-*d* experiment shown in Fig. 2b clearly demonstrate that the sequence effectively suppresses non-hyperpolarized signals thereby revealing all of the *para*-hydrogen addition products resonances. The single hydrogen addition products, 1-pentene and 2-pentene exhibit further hyperpolarized signals that result from the transfer of polarization under ALTADENA conditions to the J-coupled hydrogen atom in the 3-position [32]. These connections are only clearly visible in the OPSY experiment at δ 5.40 and 5.81 for the 2-pentene and 1-pentene isomers respectively. An NMR signal for molecular hydrogen also passes the filter and is observable at δ 4.5 due to the reversibility of the initial addition step.

Two further control experiments were collected to further test the fidelity of the OPSY-*d* method. The first of these involved the collection of a background spectrum corresponding to the point before *para*-hydrogen addition. No signal was observed in the resulting NMR spectrum. The second control was recorded after the reaction was complete. Again, no signal was observed in the resulting NMR spectrum (Fig. 2d). The sequence therefore successfully suppresses the thermal signals as desired leaving only those enhanced by the *para*-hydrogen in this methanol-d_4. Clearly hyperpolarized pentene signals can therefore be distinguished from their non-hyperpolarized counterpart using this approach.

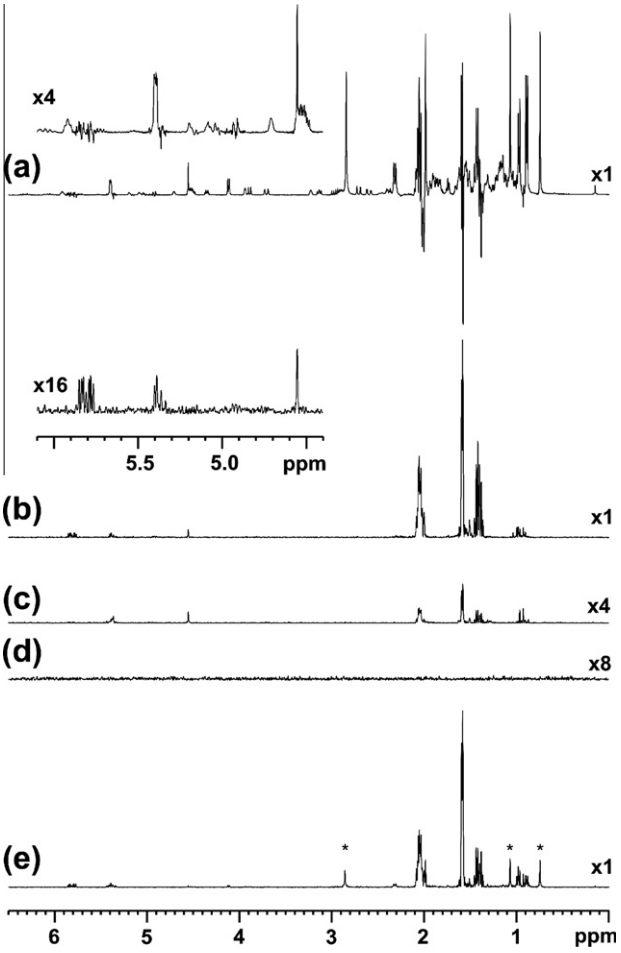

Fig. 2. ^{1}H NMR absolute value spectra (except (a) obtained for *sample A* illustrating the monitoring of a typical hydrogenation reaction with *para*-hydrogen. (a) $\pi/4$-^{1}H NMR experiment; (b) OPSY-*d* experiment revealing all *para*-hydrogen derived signals and allowing multiplet analysis; (c). OPSY-*d* experiment after reaction with no *para*-hydrogen present; (d) spectrum illustrating efficiency of thermal signal suppression; (e) OPSY-*z* experiment after and (b) revealing poorer background signal suppression (*) than OPSY-*d*.

The OPSY-*z* variant ^{1}H NMR spectrum shown in Fig. 2e contains a number of extra signals that are indicated by * arising from the additional cholesterol acetate in the sample. These results therefore reveal that the OPSY-*z* variant is less efficient at suppressing thermal magnetization.

In is also important to consider the overall magnetic efficiency of these experiments. In PASADENA, a $\pi/4$-^{1}H NMR experiment uses half of the potentially available signal from a $2I_zS_z$ starting point as demonstrated by Equation (8) for a r.f pulse of flip angle ϕ [2,33]

$$\rho_\phi = 1/2\{\cos^2(\phi)2I_zS_z+\cos(\phi)sin(\phi)(2I_zS_y+2I_yS_z) + sin^2(\phi)2I_yS_y\} \quad (8)$$

This arises because only the second term evolves into observable magnetization with the $\pi/4$ r.f. pulse maximizing its contribution. In the OPSY experiments described earlier, the initial $\pi/2$ r.f.

pulse produces no detectable signal but converts all the magnetization into $2I_yS_y$, where evolution under ω_I and ω_S proceeds. The second $\pi/2$ r.f. pulse turns the newly formed mixture of zero and double quantum coherences into terms that evolve into observable magnetization. Selection of either the zero quantum or double quantum coherence pathways therefore means that optimally either a half or a quarter of the signal is retained respectively. The OPSY-*d* experiment is half as sensitive as the OPSY-*z* variant because it selects only one of the two double quantum coherence pathways.

The spectra obtained from the OPSY experiments contain signals taken from a mixture of coherences, with different amplitudes, and hence cannot always be phased into pure absorption or dispersion. The problem is caused by signal evolution during the pulse sequence and while an echo, achieved using a further π r.f. pulse can refocus the chemical shift, this complicates the signal suppression.

This is illustrated in Fig. 3, where the result of a $\pi/4$ r.f. pulse to a sample of $Ir(CO)(P(p\text{-}MeC_6H_4)_3)_2Cl(H)_2$ reveals the anti-phase magnetization associated with the δ −6.5 hydride resonance ($2I_zS_y$). For this reason we have presented our OPSY data in absolute value. The evolution of these terms are however predictable for two spins and matching the periods of evolution to the chemical shift difference allow in-phase spectra to be collected with optimum sensitivity.

A substrate that has been hyperpolarized through the SABRE method will pass through the OPSY filter method if the states exhibit the appropriate coherences. The hyperpolarization of pyridine using *sample D* was examined using the OPSY experiments. The hyperpolarized pyridine exhibits enhanced signals in both the *ZQ* and *DQ* variants of the OPSY experiments. These possess different multiplet structure to thermal pyridine indicating that states that contribute to the zero and double quantum coherences are populated. The variant of the experiment that converts only the triple quantum (*TQ*) coherence to observable magnetization, OPSY-*t*, also generates signals after hyperpolarization of the pyridine. This demonstrates that the OPSY experiment can be used to investigate the states that are generated in hyperpolarized species formed as a result of the SABRE hyperpolarization method. The evolution of the spin system under the chemical shift and scalar coupling results in signals that have a distorted phase characteristic due to the

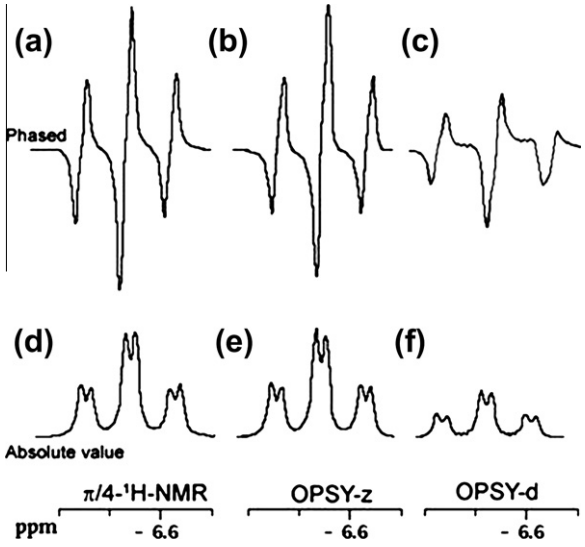

Fig. 3. Sequence sensitivity and phase properties illustrated using *sample B* for the hydride signal at δ −6.56. Optimally phased results for (a) $\pi/4$-^{1}H NMR, (b) ^{1}H OPSY-*z* and (c) ^{1}H OPSY-*d*. d, e and f show the corresponding absolute value traces with the sensitivity ratios of 1: 1: 0.5 respectively matching those predicted.

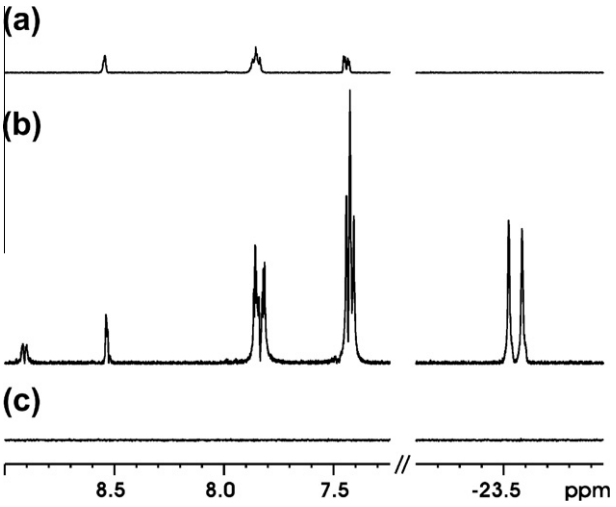

Fig. 4. The signals observed after the generation of hyperpolarized pyridine following its interaction with Crabtree's catalyst and *para*-hydrogen. The signals shown are for the hyperpolarized NMR spectra recorded with (a) OPSY-*t* and (b) OPSY-*d* experiments. The OPSY experiments suppress the signals when the system is depleted of *para*-hydrogen, shown for OPSY-*d* (c).

combination of states that contribute. For this reason the signals, presented in Fig. 4, are displayed in magnitude. The observation of the hydride (δ −23.56) and bound pyridine *ortho*-^{1}H (δ 8.91) signals in the OPSY-*d* but not in the OPSY-*t* and the bound pyridine *para*-^{1}H (δ 7.97, weak) in the OPSY-*t* but not in the OPSY-*d* are indicative of the states formed during the polarization transfer step.

5. Building block

The majority of NMR experiments that use *para*-hydrogen are based on normal NMR experiments, where the first $\pi/2$ pulse is replaced by either a $\pi/4$ r.f. pulse or by a $\pi/4$ r.f. pulse and refocusing delay. Some others feature a $\pi/4$ r.f. read pulse at the end of the pulse sequence [33,38–43].

As an example of a sequence including the OPSY building block, a gradient assisted HMBC experiment has been developed, where the first $\pi/2$-^{1}H pulse is replaced with an OPSY sequence as shown in Fig. 5. The correct choice of sequence to be employed will depend on the actual experimental requirements. For signals enhanced

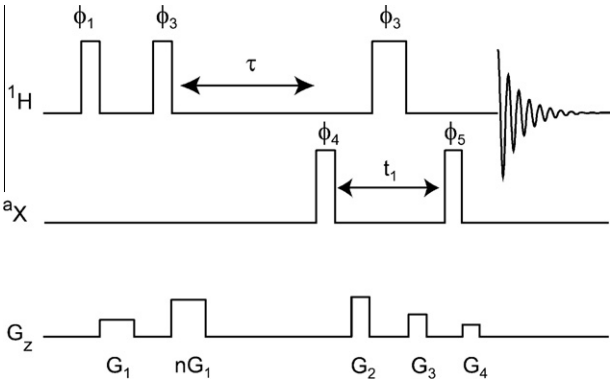

Fig. 5. Double quantum filtered HMBC experiment (OPSY-*d*-HMBC). If zero quantum filtration is desired the second gradient pulse is omitted. Phase cycle: $\phi_1 = x$, $\phi_2 = x$, $\phi_3 = x\ x\ -x\ -x$, $\phi_4 = x\ -x$, $\phi_5 = (x)_4\ (-x)_4$, $\phi_{rec} = (x\ -x)_2\ (-x\ x)_2$. Half-sine gradients were used with $G_1 = 53$ G cm^{-1}. $\delta_1 = \delta_2 = 1$ ms. G_2: G_3: G_4 50:30:40.1 for ^{13}C selection, 70:30:50.1 for ^{15}N selection and 30:30:24.3 for ^{31}P selection. $t_1 = 1/(2J_{XH})$.

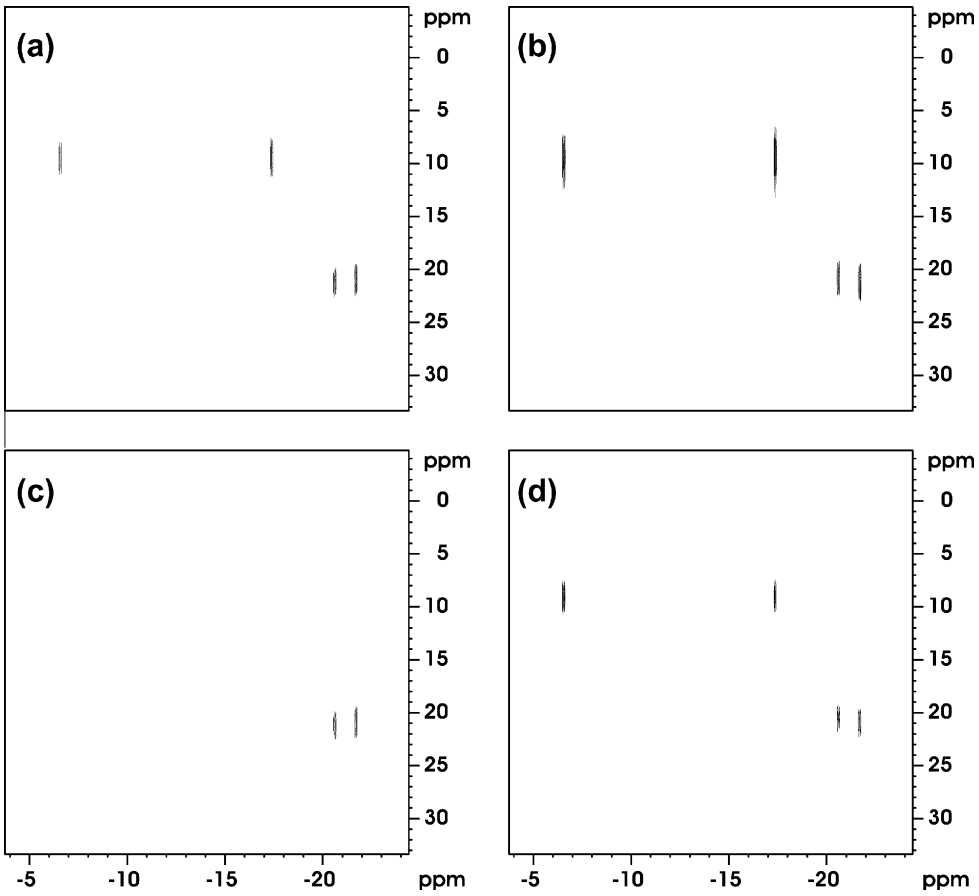

Fig. 6. A series of HMBC NMR recorded following a reaction. The sample, *sample B* with pyridine in C_6D_6 at 300 K was interrogated with $\pi/4$-^{1}H–^{31}P HMBC (right) and OPSY-*z*-HMBC experiments (left). Initially (top) both experiments exhibit two sets of enhanced signals. After the reaction has progressed both hyperpolarized and non-hyperpolarized signals appear in the $\pi/4$-experiments making it difficult to determine if the signal derives from PHIP and therefore if the reaction is occurring. In the OPSY-*z*-HMBC one set of signals are removed as the first reaction is completed and the reaction with *para*-hydrogen ceases. Only *para*-hydrogen derived protons that are coupled to ^{31}P are detected in the OPSY-*z*-HMBC experiments easing identification of the hyperpolarized signals. Spectra were recorded for 32 increments with 4 scans per increment and an acquisition time of 300 ms, no recycle delay was used. The total time taken for each experiment was 1.3 min.

using a PASADENA experiment OPSY-*d* is more efficient at thermal signal suppression while OPSY-*z* has twice the inherent sensitivity. In the present case we opt for a the OPSY-*z* because it is not susceptible to diffusion and unwanted background signal is further suppressed by the HMBC section as shown in Fig. 6. The OPSY-*d* is preferred when high performance background suppression is required while the OPSY-*t* should only be used in conjunction with experiments such as SABRE that generate higher order coherences.

Thus for homonuclear experiments OPSY-*d* will represent the more robust starting point while OPSY-*z* is superior when heteronuclear signals are to be encoded in experiments where the need for background suppression is less demanding. This situation exists when H_2O is the solvent and a ^{1}H–^{13}C HMBC dataset is collected or when a ^{1}H–^{13}P HMBC is recorded via HP couplings within the ligand sphere.

To exemplify this, *sample B* was examined over time using the ^{1}H–^{31}P OPSY-*z*-HMBC sequence and *para*-hydrogen. This sample contains the *para*-tolyl analogue of Vaska's complex, *trans*-Ir(CO)(P(*p*-$MeC_6H_4)_3)_2Cl$, and pyridine (py). After adding *para*-hydrogen, two complexes are produced, namely *trans*-Ir(CO)(P(*p*-$MeC_6H_4)_3)_2(H)_2Cl$ and Ir(py)(P(*p*-$MeC_6H_4)_3)_2(H)_2Cl$. These two complexes exhibit ^{31}P coupled ^{1}H NMR signals for the hydride ligands that resonate at δ −6.55 and δ −17.39, and δ −20.60 and δ −21.67 respectively. Under these conditions *trans*-Ir(CO)(P(*p*-$MeC_6H_4)_3)_2(H)_2Cl$ is the dominant material in solution, and *trans*-Ir(py)(P(*p*-$MeC_6H_4)_3)_2(H)_2Cl$ is only detectable through the PHIP effect.

When all of the precursor complex is consumed, the solution contains only *trans*-Ir(CO)(P(*p*-$MeC_6H_4)_3)_2(H)_2Cl$. The corresponding hydride signals that are observed for this species therefore change in appearance due to the initial creation of the two terms $+2I_yS_z + 2I_zS_y$ which then relax to thermal levels of $I_z + S_z$ during the course of the experiment. Consequently when a ^{1}H OPSY NMR spectrum is recorded, the strength of the detected signals for Ir(CO)(P(*p*-$MeC_6H_4)_3)_2(H)_2Cl$ decays with reaction time. Hydride signals are seen for the second complex, *trans*-Ir(py)(P(*p*-$MeC_6H_4)_3)_2(H)_2Cl$ throughout the experiment because they are only detected through the PHIP effect and hence remain visible until the *para*-hydrogen present in solution is consumed. They are formed via *trans*-Ir(CO)(P(*p*-$MeC_6H_4)_3)_2(H)_2Cl$ which undergoes CO dissociation to form the 16 electron complex *trans*-Ir(P(*p*-$MeC_6H_4)_3)_2(H)_2Cl$ which can be trapped by pyridine. The H_2 exchange necessary for the observed enhancement of the *trans*-Ir(py)(P(*p*-$MeC_6H_4)_3)_2(H)_2Cl$ signals proceeds via this complex.

Initially a $\pi/4$-HMBC experiment was recorded followed by the OPSY-*z*-HMBC variant. The reaction was monitored repeatedly for 2 h with no significant changes to the system between the two experiments as the combined experimental time for acquisition of both was 1.3 min.[1] The results, illustrated in Fig. 6, demonstrate that the $\pi/4$-HMBC experiment does not differentiate between signal

[1] We were able to afford a short experimental time as the usual inter-scan delay is not required, the acquisition time is short (300 ms), only four averages are needed and 32 increments provides sufficient resolution in the ^{31}P dimension.

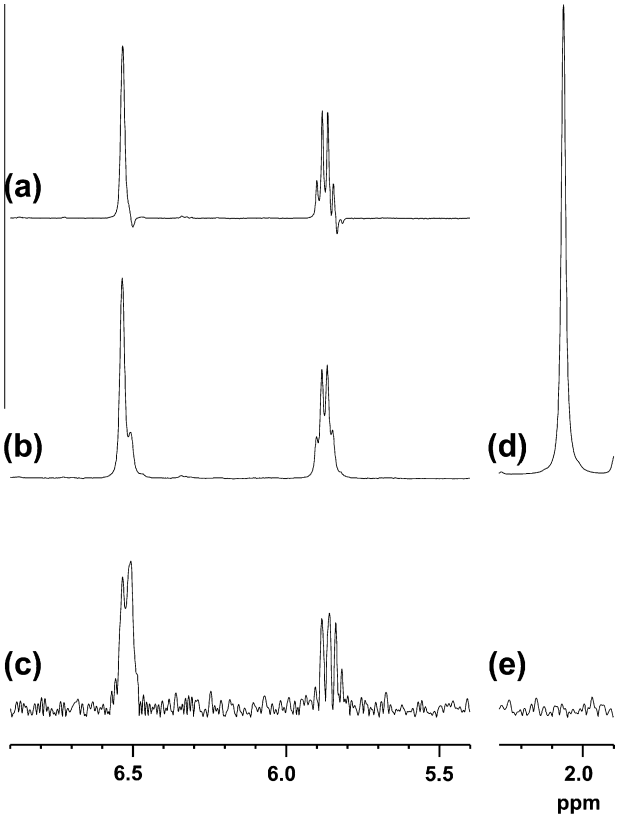

Fig. 7. NMR spectra recorded during the hydrogenation of 1-phenylpropyne to 1-phenylpropene using a standard $\pi/2$ r.f. pulse experiment using *sample C*. (a) The *para*-hydrogen enhanced signals become obscured by the thermally equilibrated signals in the reaction product as the hydrogenation progresses and (b) when the thermal signals mask the *para*-hydrogen signals entirely. The OPSY-*d* experiment shows that after recording (b) the reaction still progresses and hyperpolarized signals persist. The reaction was performed in predominantly protio-acetone and the section of spectra (b) and (c) that correspond to the solvent are shown in (d), scaled at 3% of the other experiments, and (e) respectively indicating complete suppression of the signal in the OPSY-*d* experiment. Absolute values are presented for the OPSY experiments.

types while the OPSY-*z*-HMBC experiment removes signals that do not exhibit a PHIP enhancement.

6. Solvent suppression

A significant consequence of the design of the OPSY sequences to destroy any non-hyperpolarized signals is that they correspond to a solvent suppression scheme in *para*-hydrogen enhanced NMR spectroscopy. Consequently measurements can be performed in unusual solvent systems, where deuterated solvents are expensive. Furthermore, the hydrogenation of pure reactants can also be studied, for example the hydrogenation of 1-phenylpropyne, and only signals for reaction products detected. This is demonstrated in *sample C* which contains $[(COD)Rh(dppb)]^+$ to catalyze the conversion of 0.2 mL 1-phenylpropyne to 1-phenylpropene, protio-acetone with 0.05 mL of acetone-d_6 added for locking purposes. When the reaction is monitored, strongly hyperpolarized signals at δ 5.86 and 6.52 are initially observed for the hydrogenation product. This rapidly leads to large thermal signals from the products that mask the enhanced signals. This can be seen in Fig. 7a, where there is a slight distortion to the resonances for the alkene which is absent in Fig. 7b in which the signals appear phased. Detection of the *para*-hydrogen enhancement in the latter case requires the use of OPSY to remove the congruous thermal signals. This is exemplified in Fig. 7c, where the two hyperpolarized signals are selected by the experiment while the thermal signals are filtered out. This experiment is measured in protio-acetone with a signal that is suppressed as demonstrated in Fig. 6d and e. The ability to suppress the signal from the solvent allows the gain on the receiver to be set to a high level without overloading the analogue to digital converter and therefore avoiding the associated sampling artifacts in the resulting spectra. Furthermore, provided the gradients successfully suppress the thermal signals, the maximum receiver amplification can be used allowing detection of very small hyperpolarized signals.

Table 1
E_R, assessment of the degree of solvent suppression achieved with the OPSY-*d* experiment relative to a standard *para*-hydrogen experiment according to the signal intensities, In in $(In_p/In_s)_{OPSY}/(In_p/In_s)_{\pi/4}$. $G_1 = 57$ G cm^{-1}, $\delta_1 = 3$ ms. The receiver gain was optimized for each measurement.

Solvent	E_R
THF	14,500
DCM	8500
CH_3CN	1700
DMF	1000
Xylene	490
Benzonitrile	300

A more comprehensive assessment of the selection efficiency was completed using *sample C* and a protio solvent in conjunction with an NMR tube containing a D_2O filled capillary for signal locking. The efficiency ratio (E_R) for solvent suppression was assessed by comparing the *para*-hydrogen enhanced hydride signal strengths seen for *trans*-Ir(py)(P(*p*-Me$C_6H_4)_3)_2(H)_2$Cl to residual protio signal integrals as determined in OPSY-*d* and $\pi/4$-^{1}H NMR experiments (Eq. (9)). The corresponding values of E_R are listed in Table 1. The highest value was obtained for THF, where E_R was 14,500. The corresponding OPSY-*d* spectrum is shown in Fig. 8. Less impressive, but still good, ratios were obtained with other solvents. The most probable cause for some of the low performance could be due to the presence of intermolecular dipolar interactions.

$$E_R = (In_p/In_s)_{OPSY} \Big/ (In_p/In_s)_{\pi/4} \tag{9}$$

In_p gives the integral of *para*-hydrogen signal and In_s gives the integral of solvent signal. The suffixes OPSY and $\pi/4$ indicate the experiment type.

7. Intermolecular dipolar interactions

We have described how OPSY experiments exploit *para*-hydrogen terms of the type $2I_zS_z$ that are present before the first r.f. pulse is applied. Warren et al. have reported how intermolecular dipolar interactions present in liquids result in magnetization that can be described by the term $2I_zS_z$, where the two spins involved in the interaction belong to different molecules [44]. It should therefore be expected that intermolecular dipolar interactions might contribute to signals in these experiments. Indeed with the exception of the reduced inter-scan recycle delay, OPSY sequences have the same basic structure as the CRAZED experiment used to probe dipolar intermolecular multiple quantum coherences (iMQCs). Control experiments recorded before *para*-hydrogen addition or after depletion will identify artifacts that may be caused by iMQCs which can also be characterized by varying the concentration on which they are dependent. These interferences can be suppressed using gradients at the magic angle [44] or minimized using high repetition rates.

8. Conclusions and remarks

We have shown how the OPSY filtering sequence that is based on coherence transfer pathway selection can be employed to selec-

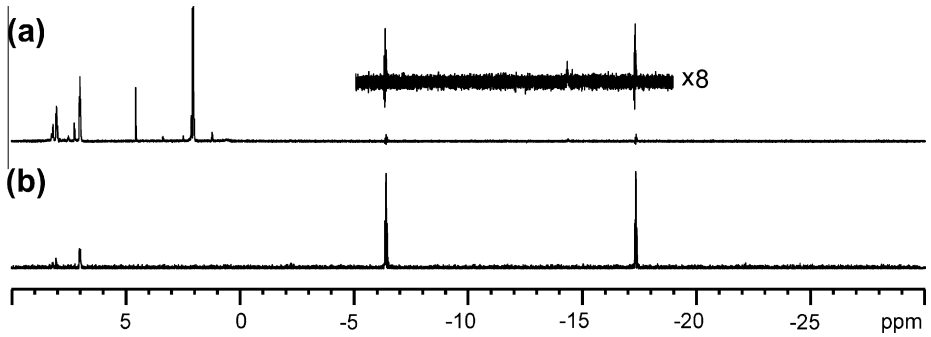

Fig. 8. Spectra of a sample of the *para*-tolyl analogue of Vaskás complex after adding three atmospheres of *para*-hydrogen. Hydrides signals at δ −6.56 and −17.35 are detected. In the $\pi/4$-^{1}H NMR experiment, (a), these hydrides are barely seen due to the severe dynamic range problems. In the OPSY-*d* experiment, (b), both hydrides can be clearly seen. Sine shaped gradients were used: G_1 = 57 G cm^{-1}, δ_1 = 3 ms. The top trace is presented in absolute value mode. Two strong solvent contaminants are marked with asterisks. Note only *para*-hydrogen derived signals are present in the OPSY-*d* experiment.

tively detect magnetization derived from *para*-hydrogen. Procedures based on quantum coherence selection have been evaluated for *para*-hydrogen addition products. The zero quantum variant, OPSY-*z*, exhibits inferior suppression compared to the other sequences which contain a second PFG. This additional PFG dephases any signals deriving from residual thermal magnetization which was unaffected by the first r.f. pulse. The zero quantum variant is however more sensitive since it converts 50% of the available magnetization into an observable form in contrast to the 25% level for OPSY-*d* and since it only involves a single gradient pulse it is less susceptible to turbulence, convection and changes in the chemical composition during the sequence. Nonetheless, in spite of its lower inherent sensitivity, we consider the double quantum variant to be best suited for routine use due to its superior solvent suppression efficiency. Artifacts that survive the OPSY-*d* and OPSY-*z* filters can be easily identified by recording control experiments either prior to the addition of *para*-hydrogen or after reaction.

9. Future work

The two OPSY filtration sequences exploit the $2I_zS_z$ magnetization which is produced by the hyperpolarization technique. This form of magnetization is not exclusive to *para*-hydrogen derived hyperpolarization, also being created with Chemically and Photochemically Induced Dynamic Nuclear Polarization (CIDNP, PHDNP) [22,45]. These techniques could potentially benefit even more substantially from the OPSY approach because while *para*-hydrogen experiments suffer from a moderate degree of signal overlap, when CIDNP is used in the study of proteins severe spectral overcrowding often occurs. The OPSY sequences may also be exploited in the study of reaction kinetics using sequences analogous to those of the DYPAS [46] and ROCHESTER experiments. This allows the rate of reaction to be determined and the removal of thermal signals through the use of the OPSY will improve the accuracy of the results.

Acknowledgments

The authors would like to thank Prof. G.A. Morris (University of Manchester) and Dr. D.C. Williamson (University of York) for their useful comments. RWA thanks the BBSRC and YNI limited for a PhD CASE studentship. We also wish to thank the Basic Technology programme, the EPSRC and the University of York for funding this research.

Appendix A. Supplementary material

Supplementary data associated with this article can be found, in the online version, at doi:10.1016/j.jmr.2010.10.002.

References

[1] T.C. Eisenschmid, R.U. Kirss, P.P. Deutsch, S.I. Hommeltoft, R. Eisenberg, J. Bargon, R.G. Lawler, A.L. Balch, Para hydrogen induced polarization in hydrogenation reactions, J. Am. Chem. Soc. 109 (1987) 8089–8091.
[2] C.R. Bowers, D.P. Weitekamp, Para-hydrogen and synthesis allow dramatically enhanced nuclear alignment, J. Am. Chem. Soc. 109 (1987) 5541–5542.
[3] C.R. Bowers, D.P. Weitekamp, Transformation of symmetrization order to nuclear-spin magnetization by chemical-reaction and nuclear-magnetic-resonance, Phys. Rev. Lett. 57 (1986) 2645–2648.
[4] L.T. Kuhn, J. Bargon, Transfer of parahydrogen-induced hyperpolarization to heteronuclei, in: In Situ NMR Methods in Catalysis, 2007, pp. 25–68.
[5] E.Y. Chekmenev, J. Hovener, V.A. Norton, K. Harris, L.S. Batchelder, P. Bhattacharya, B.D. Ross, D.P. Weitekamp, PASADENA hyperpolarization of succinic acid for MRI and NMR spectroscopy, J. Am. Chem. Soc. 130 (2008) 4212–4213.
[6] S.B. Duckett, C.J. Sleigh, Applications of the parahydrogen phenomenon: a chemical perspective, Prog. Nucl. Magn. Reson. Spectrosc. 34 (1999) 71–92.
[7] C. Godard, S.B. Duckett, S. Polas, R. Tooze, A.C. Whitwood, Detection of intermediates in cobalt-catalyzed hydroformylation using para-hydrogen-induced polarization, J. Am. Chem. Soc. 127 (2005) 4994–4995.
[8] A. Viale, D. Santelia, R. Napolitano, R. Gobetto, W. Dastru, S. Aime, The detection of PHIP effects allows new insights into the mechanism of olefin isomerisation during catalytic-hydrogenation, Eur. J. Inorg. Chem. (2008) 4348–4351.
[9] M. Stephan, O. Kohlmann, H.G. Niessen, A. Eichhorn, J. Bargon, Carbon-13 PHIP NMR spectra and polarization transfer during the homogeneous hydrogenation of alkynes with parahydrogen, Magn. Reson. Chem. 40 (2002) 157–160.
[10] L.T. Kuhn, U. Bommerich, J. Bargon, Transfer of parahydrogen-induced hyperpolarization to F-19, J. Phys. Chem. A 110 (2006) 3521–3526.
[11] J. Lopez-Serrano, S.B. Duckett, S. Aiken, K.Q.A. Lenero, E. Drent, J.P. Dunne, D. Konya, A.C. Whitwood, A para-hydrogen investigation of palladium-catalyzed alkyne hydrogenation, J. Am. Chem. Soc. 129 (2007) 6513–6527.
[12] H. Johannesson, O. Axelsson, M. Karlsson, Transfer of para-hydrogen spin order into polarization by diabatic field cycling, C. R. Phys. 5 (2004) 315–324.
[13] M. Goldman, H. Johannesson, Conversion of a proton pair para order into carbon-13 polarization by rf irradiation, for use in MRI, C. R. Phys. 6 (2005) 575–581.
[14] J. Wolber, F. Ellner, B. Fridlund, A. Gram, H. Johannesson, G. Hansson, L.H. Hansson, M.H. Lerche, S. Mansson, R. Servin, M. Thaning, K. Golman, J.H. Ardenkjaer-Larsen, Generating highly polarized nuclear spins in solution using dynamic nuclear polarization, Nuclear Instruments & Methods in Physics Research Section a-Accelerators Spectrometers Detectors and Associated Equipment 526 (2004) 173–181.
[15] H. Johanneson, S. Macholl, J.H. Ardenkjaer-Larsen, Dynamic nuclear polarization of 1-carbon-13 pyruvic acid at 4.6 T, J. Magn. Reson. 197 (2009) 167–175.
[16] K. Golman, J.S. Petersson, Metabolic imaging and other applications of hyperpolarized carbon-13, Academic Radiology 13 (2006) 932–942.
[17] E.Y. Chekmenev, V.A. Norton, D.P. Weitekamp, P. Bhattacharya, Hyperpolarized H-1 NMR employing low gamma nucleus for spin polarization storage, J. Am. Chem. Soc. 131 (2009) 3164–3165.
[18] R.W. Adams, J.A. Aguilar, K.D. Atkinson, M.J. Cowley, P.I.P. Elliott, S.B. Duckett, G.G.R. Green, I.G. Khazal, J. Lopez-Serrano, D.C. Williamson, Reversible Interactions with para-hydrogen enhance NMR sensitivity by polarization transfer, Science 323 (2009) 1708–1711.
[19] R.W. Adams, S.B. Duckett, R.A. Green, D.C. Williamson, G.G.R. Green, A theoretical basis for spontaneous polarization transfer in non-hydrogenative parahydrogen-induced polarization, J. Chem. Phys. 131 (2009) 194505.
[20] P. Hubler, R. Giernoth, G. Kummerle, J. Bargon, Investigating the kinetics of homogeneous hydrogenation reactions using PHIPNMR spectroscopy, J. Am. Chem. Soc. 121 (1999) 5311–5318.

[21] S.B. Duckett, N.J. Wood, Parahydrogen-based NMR methods as a mechanistic probe in inorganic chemistry, Coord. Chem. Rev. 252 (2008) 2278–2291.
[22] R. Boelens, A. Podoplelov, R. Kaptein, Separation of net polarization and multiplet effect in coupled spin systems by two-dimensional cidnp, J. Magn. Reson. 69 (1986) 116–123.
[23] A. Eichhorn, A. Koch, J. Bargon, In situ PHIP NMR – a new tool to investigate hydrogenation mediated by colloidal catalysts, Journal of Molecular Catalysis a – Chemical 174 (2001) 293–295.
[24] H.G. Niessen, D. Schleyer, S. Wiemann, J. Bargon, S. Steines, B. Driessen-Hoelscher, In situ PHIP NMR studies during the stereoselective hydrogenation of sorbic acid with a Cp^{*} Ru (+) catalyst, Magn. Reson. Chem. 38 (2000) 747–750.
[25] A. Harthun, R. Giernoth, C.J. Elsevier, J. Bargon, Rhodium- and palladium-catalysed proton exchange in styrene detected in situ by para-hydrogen induced polarization, Chem. Commun. (Cambridge, UK) (1996) 2483–2484.
[26] J. Lopez-Serrano, S.B. Duckett, A. Lledos, Palladium-catalyzed hydrogenation: detection of palladium hydrides. A joint study using para-hydrogen-enhanced NMR spectroscopy and density functional theory, J. Am. Chem. Soc. 128 (2006) 9596–9597.
[27] J.P. Dunne, S. Aiken, S.B. Duckett, D. Konya, K.Q.A. Lenero, E. Drent, Detection and reactivity of Pd((C8H14)PCH2CH2P(C8H14))(CHPhCH2Ph)(H) as determined by parahydrogen-enhanced NMR spectroscopy, J. Am. Chem. Soc. 126 (2004) 16708–16709.
[28] J.A. Aguilar, P.I.P. Elliott, J. Lopez-Serrano, R.W. Adams, S.B. Duckett, Only *para*-hydrogen spectroscopy (OPSY), a technique for the selective observation of para-hydrogen enhanced NMR signals, Chem. Commun. (Cambridge, UK) (2007) 1183–1185.
[29] R. Kandiah, Applications of the Parahydrogen Phenomenon in the Biological Field, Ph.D Thesis, University of York, 2007.
[30] M.J. Burk, R.H. Crabtree, A convenient general-synthesis of trans-[IrCl(CO)$(PR_3)_2$], Inorg. Chem. 25 (1986) 931–932.
[31] D. Canet, C. Aroulanda, P. Mutzenhardt, S. Aime, R. Gobetto, F. Reineri, Para-hydrogen enrichment and hyperpolarization, Concepts Mag. Reson. Part A 28A (2006) 321–330.
[32] M.G. Pravica, D.P. Weitekamp, Net NMR alignment by adiabatic transport of para-hydrogen addition products to high magnetic field, Chem. Phys. Lett. 145 (1988) 255–258.
[33] J. Natterer, J. Bargon, Parahydrogen induced polarization, Prog. Nucl. Magn. Reson. Spectrosc. 31 (1997) 293–315.
[34] O.W. Sorensen, G.W. Eich, M.H. Levitt, G. Bodenhausen, R.R. Ernst, Product operator-formalism for the description of NMR pulse experiments, Prog. Nucl. Magn. Reson. Spectrosc. 16 (1983) 163–192.
[35] P.J. Hore, J.A. Jones, S. Wimperis, NMR: The Toolkit, Oxford University Press, 2000.
[36] J. Keeler, R.T. Clowes, A.L. Davis, E.D. Laue, Pulsed field gradients – theory and practice, Nucl. Mag. Reson. C 239 (1994) 145.
[37] A. Bax, P.G. Dejong, A.F. Mehlkopf, J. Smidt, Separation of the different orders of NMR multiple-quantum transitions by the use of pulsed field gradients, Chem. Phys. Lett. 69 (1980) 567.
[38] T.C. Eisenschmid, J. McDonald, R. Eisenberg, R.G. Lawler, INEPT in a chemical way – polarization transfer from para-hydrogen to P-31 by oxidative addition and dipolar relaxation, J. Am. Chem. Soc. 111 (1989) 7267–7269.
[39] H. Sengstschmid, R. Freeman, J. Barkemeyer, J. Bargon, A new excitation sequence to observe the PASADENA effect, Journal of Magnetic Resonance Series A 120 (1996) 249–257.
[40] S.B. Duckett, C.L. Newell, R. Eisenberg, More than INEPT – parahydrogen and INEPT+ Give unprecedented resonance enhancement to carbon-13 by direct H-1 polarization transfer, J. Am. Chem. Soc. 115 (1993) 1156–1157.
[41] S.B. Duckett, G.K. Barlow, M.G. Partridge, B.A. Messerle, Rapid characterization of rhodium dihydrides by nuclear-magnetic-resonance spectroscopy using indirect 2-dimensional methods and para-hydrogen, Journal of the Chemical Society-Dalton Transactions (1995) 3427–3429.
[42] J. Natterer, J. Barkemeyer, J. Bargon, Determination of J(CC) coupling constants using parahydrogen-induced polarization, Journal of Magnetic Resonance Series A 123 (1996) 253–256.
[43] M. Haake, J. Natterer, J. Bargon, Efficient NMR pulse sequences to transfer the parahydrogen-induced polarization to hetero nuclei, J. Am. Chem. Soc. 118 (1996) 8688–8691.
[44] W.S. Warren, W. Richter, A.H. Andreotti, B.T. Farmer, Generation of impossible cross-peaks between bulk water and biomolecules in solution NMR, Science 262 (1993) 2005–2009.
[45] R. Kaptein, L.J. Oosterho, Chemically induced dynamic nuclear polarization, Chem. Phys. Lett. 4 (1969) 195.
[46] M.S. Chinn, R. Eisenberg, Rates of catalytic-hydrogenation estimated spectroscopically through enhanced resonances, J. Am. Chem. Soc. 114 (1992) 1908–1909.